Prepared for submission to JHEP

The Drell-Yan process with pions and polarized nucleons

S. Bastami[a] **L. Gamberg**[b] **B. Parsamyan**[c,d] **B. Pasquini**[e,f] **A. Prokudin**[b,g] **P. Schweitzer**[a]

[a] *Department of Physics, University of Connecticut, Storrs, CT 06269, U.S.A.*
[b] *Division of Science, Penn State Berks, Reading, PA 19610, USA*
[c] *CERN, 1211 Geneva 23, Switzerland*
[d] *INFN, Sezione di Torino, 10125 Torino, Italy*
[e] *Dipartimento di Fisica, Universitá degli Studi di Pavia, Italy*
[f] *Istituto Nazionale di Fisica Nucleare, Sezione di Pavia, Italy*
[g] *Thomas Jefferson National Accelerator Facility, Newport News, VA 23606, U.S.A.*

E-mail: saman.bastami@uconn.edu, lpg10@psu.edu, bakur@cern.ch, barbara.pasquini@unipv.it, prokudin@jlab.org, peter.schweitzer@uconn.edu

Abstract: The Drell-Yan process provides important information on the internal structure of hadrons including transverse momentum dependent parton distribution functions (TMDs). In this work we present calculations for the Drell-Yan process from collisions of pions and polarized protons at leading twist. The non-perturbative input for the TMDs is taken from the light-front constituent quark model, the spectator model, and available parametrizations of TMDs extracted from the experimental data. Our results are compatible with the first experimental information, and will help to interpret the data from ongoing experiments, as well as allow one to quantitatively assess these models in the future when more precise data will become available.

1 Introduction

The Drell-Yan (DY) process with pions and nucleons provides important information on the structure of pion and nucleon. The DY differential cross section in the region of low transverse momentum, q_T, of the produced lepton anti-lepton pair is subject to the transverse momentum dependent factorization [1]. The corresponding transverse momentum dependent parton distribution functions (TMDs) [2] in the description of DY at low q_T provide essential information on correlations between transverse parton momenta and parton or nucleon spin, and describe the three-dimensional structure of hadrons. Early theoretical studies of TMDs in hadron production in proton-proton processes [3–5] were followed by systematic investigations in semi-inclusive deep-inelastic scattering (SIDIS) [6–9] and DY [10–12] (also fragmentation functions [13] enter the description of SIDIS). The basis for these descriptions are QCD factorization theorems [1, 2, 14–22].

One of the challenges when interpreting pion-induced DY data is the limited knowledge of the pion structure. At twist-2 the process is described by the proton TMDs: unpolarized distribution $f^a_{1,p}$, transversity distribution $h^a_{1,p}$, Sivers distribution function $f^{\perp a}_{1T,p}$, Boer-Mulders distribution $h^{\perp a}_{1,p}$, Kotzinian-Mulders distribution $h^{\perp a}_{1L,p}$, and "pretzelosity" distribution $h^{\perp a}_{1T,p}$, and pion TMDs: unpolarized distribution $f^a_{1,\pi}$, Boer-Mulders distribution $h^{\perp a}_{1,\pi}$.

On the proton side, $f^a_{1,p}$ both collinear and TMD are well-known [23–33]. Based on global QCD analyses of data, parametrizations are available also for $f^{\perp a}_{1T,p}$, $h^a_{1,p}$, $h^{\perp a}_{1,p}$, $h^{\perp a}_{1T,p}$ [34–38]. Only $h^{\perp a}_{1L,p}$ has not yet been extracted, though it can be described based on $h^a_{1,p}$ in the so-called Wandzura-Wilczek- (WW-)type approximation which is compatible with available data [39]. On the pion side the situation is different. While extractions of $f^a_{1,\pi}$ exist [40–45], no results on $h^{\perp a}_{1,\pi}$ are available. This constitutes a "bottleneck" if one would like to describe the COMPASS data [46] based solely on phenomenological extractions since $h^{\perp a}_{1,\pi}$ is relevant for the majority of observables in the pion-induced polarized DY process at leading twist. In this situation we will resort to model studies of the pion Boer-Mulders function $h^{\perp a}_{1,\pi}$.

An important goal of theoretical studies in models is to describe hadron structure at a low initial scale $\mu_0 < 1\,\text{GeV}$ in terms of effective constituent quark degrees of freedom. This approach has been effective and successful in describing various hadronic properties in terms of "valence-quark degrees of freedom." The underlying idea is that at a low hadronic scale μ_0, e.g., the properties of the nucleon can be modelled in terms of wave functions of u and d quarks, and similarly the properties of, e.g., π^- in terms of the wave functions of valence $\bar{u}$ and d quarks. It is an interesting task in itself to apply such a framework to the description of hadronic properties like TMDs. This has been done in a variety of complementary approaches including spectator models (SPMs) [47–51], light-front constituent quark model (LFCQM) [52–59] or bag models [60–64]. Phenomenological studies in the LFCQM showed that within a model accuracy of 20-30% a good description of SIDIS and unpolarized DY data can be obtained [55–57].

The goal of the present work is to study the spin and azimuthal asymmetries in the DY process with pions and polarized nucleons, and present calculations for all twist-2 asymmetries. We use available phenomenological extractions of TMDs and calculations from two well-established constituent-quark-models (CQM), the LFCQM and the SPM. Other studies in models, perturbative QCD and lattice QCD of the pion-induced DY or relevant TMDs have been reported [65–71].

Several features distinguish our work from other studies. First, we use two CQM frameworks with diverse descriptions of the pion and nucleon structure. Second, we describe all leading-twist observables in pion-induced polarized DY entirely in the models. Third, we supplement our studies with "hybrid calculations", where we use as much as possible information from phenomenological analyses, and only the Boer-Mulders function $h^{\perp a}_{1,\pi}$ is taken from models. Overall, we present up to four different calculations for each observable. This allows us to critically assess model dependence, and uncertainties in our approach. Where available the results are compared to the COMPASS DY data [46].

TMD evolution [2] plays an important role in interpreting the data and understanding of TMDs. In Refs. [72, 73] TMD evolution was shown to be important for the description of the pion-induced unpolarized DY cross-sections. TMD evolution has been studied for the COMPASS DY data and asymmetries also in Refs. [71, 73–76]. QCD evolution is particularly important when applying CQM results obtained at a low initial scale to the description of high-energy processes. Given the precision of current data and accuracy of models, we will content ourselves with an approximate evolution method shown to provide good estimates of evolution effects in prior studies.

Our results serve several purposes. They help to interpret in their full complexity the first COMPASS data [46] on the pion-induced polarized DY process, and in this way deepen the understanding of the QCD description of deep-inelastic processes in terms of TMDs. They also provide quantitative tests of the application of CQMs to the description of pion and nucleon structure.

2 Drell-Yan process with pions and polarized protons

In this section we briefly review the DY formalism, and provide the description of the DY structure functions in our approach.

2.1 Structure functions

In the tree-level description a dilepton l, l' is produced from the annihilation of a quark and anti-quark carrying the fractions x_π, x_p of the longitudinal momenta of respectively the pion and the proton. The process is shown in the Collins-Soper frame in Fig. 1. In the case of pions colliding with polarized protons the DY cross section is described in terms of 6 structure functions [12]

$$
\begin{aligned}
F_{UU}^{1} &= \mathcal{C}\Big[f_{1,\pi}^{\bar a}\, f_{1,p}^{a}\Big], \\
F_{UU}^{\cos 2\phi} &= \mathcal{C}\Big[\frac{2(\hat{\boldsymbol h}\cdot\vec{\boldsymbol k}_{T\pi})(\hat{\boldsymbol h}\cdot\vec{\boldsymbol k}_{Tp})-\vec{\boldsymbol k}_{T\pi}\cdot\vec{\boldsymbol k}_{Tp}}{M_\pi\, M_p}\, h_{1,\pi}^{\perp\bar a}\, h_{1,p}^{\perp a}\Big], \\
F_{UL}^{\sin 2\phi} &= \mathcal{C}\Big[\frac{2(\hat{\boldsymbol h}\cdot\vec{\boldsymbol k}_{T\pi})(\hat{\boldsymbol h}\cdot\vec{\boldsymbol k}_{Tp})-\vec{\boldsymbol k}_{T\pi}\cdot\vec{\boldsymbol k}_{Tp}}{M_\pi\, M_p}\, h_{1,\pi}^{\perp\bar a}\, h_{1L,p}^{\perp a}\Big], \\
F_{UT}^{\sin\phi_S} &= \mathcal{C}\Big[\frac{\hat{\boldsymbol h}\cdot\vec{\boldsymbol k}_{Tp}}{M_p}\, f_{1,\pi}^{\bar a}\, f_{1T,p}^{\perp a}\Big], \\
F_{UT}^{\sin(2\phi-\phi_S)} &= \mathcal{C}\Big[\frac{\hat{\boldsymbol h}\cdot\vec{\boldsymbol k}_{T\pi}}{M_\pi}\, h_{1,\pi}^{\perp\bar a}\, h_{1,p}^{a}\Big], \\
F_{UT}^{\sin(2\phi+\phi_S)} &= \mathcal{C}\Big[\frac{2(\hat{\boldsymbol h}\cdot\vec{\boldsymbol k}_{Tp})[2(\hat{\boldsymbol h}\cdot\vec{\boldsymbol k}_{T\pi})(\hat{\boldsymbol h}\cdot\vec{\boldsymbol k}_{Tp})-\vec{\boldsymbol k}_{T\pi}\cdot\vec{\boldsymbol k}_{Tp}]-\vec{\boldsymbol k}_{Tp}^2(\hat{\boldsymbol h}\cdot\vec{\boldsymbol k}_{T\pi})}{2\, M_\pi\, M_p^2}\, h_{1,\pi}^{\perp\bar a}\, h_{1T,p}^{\perp a}\Big].
\end{aligned}
\tag{2.1}
$$

The subscripts indicate the hadron polarization which can be unpolarized U (pions, protons), longitudinally L, or transversely T polarized (protons). The azimuthal angles ϕ, ϕ_S are defined in Fig. 1, where the unit vector $\hat{\boldsymbol h} = \boldsymbol q_T/q_T$ points along x-axis. Notice that in the Collins-Soper frame the dilepton is at rest, and each incoming hadron carries the transverse momentum $\boldsymbol q_T/2$, see Fig. 1. The convolution integrals in Eq. (2.1) are defined [12] as

$$
\mathcal{C}[\omega\, f_\pi^{\bar a}\, f_p^{a}] = \frac{1}{N_c}\sum_a e_a^2 \int d^2\boldsymbol k_{T\pi}\, d^2\boldsymbol k_{Tp}\, \delta^{(2)}(\boldsymbol q_T-\boldsymbol k_{T\pi}-\boldsymbol k_{Tp})\,\omega\, f_\pi^{\bar a}(x_\pi,\boldsymbol k_{T\pi}^2) f_p^{a}(x_p,\boldsymbol k_{Tp}^2)\,, \tag{2.2}
$$

where ω, a function of the transverse momenta $\boldsymbol k_{T\pi}$, $\boldsymbol k_{Tp}$ and $\boldsymbol q_T$, projects out the corresponding azimuthal angular dependence. The sum over $a = u,\, \bar u,\, d,\, \bar d,\, \dots$ includes the active flavors.

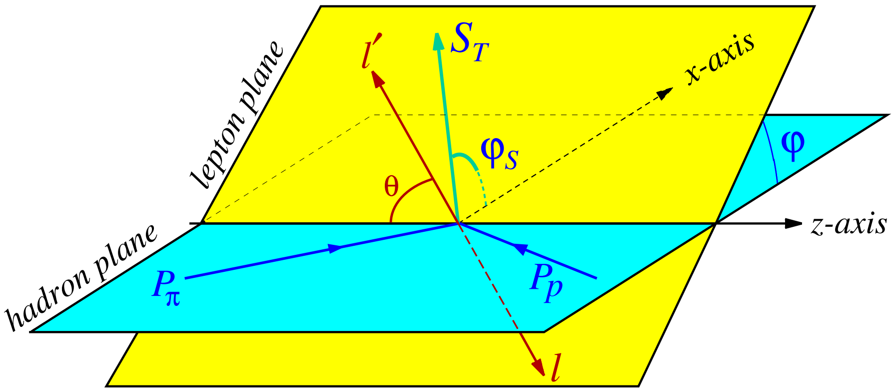

Figure 1. The DY process in the Collins-Soper frame where the pion and the proton come in with different momenta P_π, P_p, but each carries the same transverse momentum $\frac{1}{2}\boldsymbol{q}_T$, and the produced lepton pair is at rest. The angle ϕ describes the inclination of the leptonic frame with respect the hadronic plane, and ϕ_S is the azimuthal angle of the transverse-spin vector of the proton.

This partonic interpretation of DY is based on a TMD factorization [1, 2] and valid at $q_T \ll Q$. In our work we will focus on the description of asymmetries of the kind

$$A_{XY}^{\text{weight}}(x_\pi, x_p, q_T) = \frac{F_{XY}^{\text{weight}}(x_\pi, x_p, q_T)}{F_{UU}^{1}(x_\pi, x_p, q_T)}. \tag{2.3}$$

In such asymmetries there is tendency for various types of higher order corrections to largely cancel out [77–83]. Thus, when applied to the description of asymmetries, the tree-level formalism used in this work can be expected to give a good approximation.

The Q^2 dependence of the structure functions and asymmetries will often not be explicitly indicated for brevity, as in Eq. (2.3). In the following we will display results for the asymmetries as functions of one of the variables x_π, x_p, q_T. It is then understood that the structure functions are integrated over the respectively other variables within the acceptance of the experiment, keeping in mind that x_π, x_p are connected to each other by $x_\pi\, x_p = Q^2/s$.

2.2 The model for transverse momentum dependence of TMDs

The q_T-dependence of the unpolarized DY cross section can be well described [84, 85] in terms of the Gaussian Ansatz. We will utilize the following parametrizations [39] for TMDs

$$\begin{aligned}
f_h^a(x_h, \boldsymbol{k}_{Th}) &= f_h^a(x_h)\, \frac{e^{-\boldsymbol{k}_{Th}^2/\langle k_{Th}^2\rangle_{f_h}}}{\pi\,\langle k_{Th}^2\rangle_{f_h}}\,, && f_h^a = f_{1,p}^a,\ f_{1,\pi}^a,\ h_{1,p}^a,\\
f_h^a(x_h, \boldsymbol{k}_{Th}) &= f_h^{(1)a}(x_h)\, \frac{2M_h^2}{\pi\langle k_{Th}^2\rangle_{f_h}^2}\, e^{-\boldsymbol{k}_{Th}^2/\langle k_{Th}^2\rangle_{f_h}}, && f_h^a = f_{1T,p}^{\perp a},\ h_{1,p}^{\perp a},\ h_{1,\pi}^{\perp a},\ h_{1L,p}^{\perp a},\\
f_h^a(x_h, \boldsymbol{k}_{Th}) &= f_h^{(2)a}(x_h)\, \frac{2M_h^4}{\pi\langle k_{Th}^2\rangle_{f_h}^3}\, e^{-\boldsymbol{k}_{Th}^2/\langle k_{Th}^2\rangle_{f_h}}, && f_h^a = h_{1T,p}^{\perp q},
\end{aligned} \tag{2.4}$$

where transverse moments of TMDs are defined as

$$f_h^{(n)}(x_h) = \int \mathrm{d}^2\boldsymbol{k}_{Th} \left(\frac{\boldsymbol{k}_{Th}^2}{2M_h^2}\right)^n f_h(x_h, \boldsymbol{k}_{Th})\,. \tag{2.5}$$

Using the Ansatz (2.4) one obtains for the convolution integrals in Eq. (2.1) the following results

$$
\begin{aligned}
F_{UU}^{1}(x_\pi, x_p, q_T) &= \frac{1}{N_c}\sum_a e_a^2\; f_{1,\pi}^a(x_\pi)\; f_{1,p}^{\bar a}(x_p)\; \frac{e^{-q_T^2/\langle q_T^2\rangle}}{\pi\;\langle q_T^2\rangle}, \\
F_{UT}^{\sin\phi_S}(x_\pi, x_p, q_T) &= \frac{1}{N_c}\sum_a e_a^2\; f_{1,\pi}^a(x_\pi)\; f_{1T,p}^{\perp(1)\bar a}(x_p)\; 2M_p\; \frac{q_T}{\langle q_T^2\rangle}\; \frac{e^{-q_T^2/\langle q_T^2\rangle}}{\pi\;\langle q_T^2\rangle}, \\
F_{UT}^{\sin(2\phi-\phi_S)}(x_\pi, x_p, q_T) &= -\frac{1}{N_c}\sum_a e_a^2\; h_{1,\pi}^{\perp(1)a}(x_\pi)\; h_{1,p}^{\bar a}(x_p)\; 2M_\pi\; \frac{q_T}{\langle q_T^2\rangle}\; \frac{e^{-q_T^2/\langle q_T^2\rangle}}{\pi\;\langle q_T^2\rangle}, \\
F_{UU}^{\cos 2\phi}(x_\pi, x_p, q_T) &= \frac{1}{N_c}\sum_a e_a^2\; h_{1,\pi}^{\perp(1)a}(x_\pi)\; h_{1,p}^{\perp(1)\bar a}(x_p)\; 4M_\pi M_p\; \frac{q_T^2}{\langle q_T^2\rangle^2}\; \frac{e^{-q_T^2/\langle q_T^2\rangle}}{\pi\;\langle q_T^2\rangle}, \\
F_{UL}^{\sin 2\phi}(x_\pi, x_p, q_T) &= -\frac{1}{N_c}\sum_a e_a^2\; h_{1,\pi}^{\perp(1)a}(x_\pi)\; h_{1L,p}^{\perp(1)\bar a}(x_p)\; 4M_\pi M_p\; \frac{q_T^2}{\langle q_T^2\rangle^2}\; \frac{e^{-q_T^2/\langle q_T^2\rangle}}{\pi\;\langle q_T^2\rangle}, \\
F_{UT}^{\sin(2\phi+\phi_S)}(x_\pi, x_p, q_T) &= -\frac{1}{N_c}\sum_a e_a^2\; h_{1,\pi}^{\perp(1)a}(x_\pi)\; h_{1T,p}^{\perp(2)\bar a}(x_p)\; 2M_\pi M_p^2\; \frac{q_T^3}{\langle q_T^2\rangle^3}\; \frac{e^{-q_T^2/\langle q_T^2\rangle}}{\pi\;\langle q_T^2\rangle}, \qquad (2.6)
\end{aligned}
$$

where the index $a = u,\, \bar u,\, d,\, \bar d,\, \ldots$ and the mean transverse momenta $\langle q_T^2\rangle$ are defined in each case as the sums of the mean transverse momenta of the corresponding TMDs, e.g. in (2.6) in the first equation $\langle q_T^2\rangle = \langle k_{T\pi}^2\rangle_{f_{1,\pi}} + \langle k_{Tp}^2\rangle_{f_{1,p}}$, in the second equation $\langle q_T^2\rangle = \langle k_{T\pi}^2\rangle_{f_{1,\pi}} + \langle k_{Tp}^2\rangle_{f_{1T,p}^{\perp}}$, etc.

In the Gaussian model the expressions can be written in different ways. In Eq. (2.6) we have chosen a specific way consistent with Operator Product Expansion for TMDs, such that TMDs are directly written in terms of the corresponding collinear functions. In these expression it is evident that the asymmetries decrease if the transverse parton momentum distributions are broadened, which is qualitatively expected at higher energies, as we shall discuss in more detail below. This approach has been found practical in previous studies [39, 56, 57].

2.3 TMDs extracted from experimental data

In order to compute leading-twist structure functions in pion-induced DY the knowledge of the proton and pion TMDs $f_{1,p}^a$, $f_{1,\pi}^a$, $f_{1T,p}^{\perp a}$, $h_{1,p}^a$, $h_{1,p}^{\perp a}$, $h_{1T,p}^{\perp a}$, $h_{1L,p}^{\perp a}$, $h_{1,\pi}^{\perp a}$ is required, which we list here in the order from the best to the least known TMD, see Fig. 2 for an overview.

Such a classification is to some extent subjective, though it is undisputed that the collinear proton distributions $f_{1,p}^a(x_p)$ are best known [25–28] thanks to DIS, DY and other data. We will

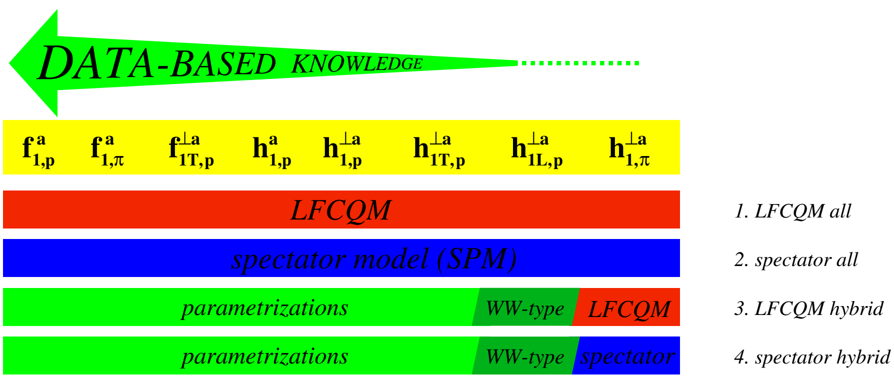

Figure 2. TMDs entering the pion-induced polarized DY process at leading twist in the order from the phenomenologically best to least known, and the approaches used in this work, see text.

utilize the MSTW extraction of $f^a_{1,p}(x_p)$ [26] for comparison with models and our calculations. The unpolarized TMDs $f^a_{1,p}(x_p, \boldsymbol{k}_{Tp})$ have been studied and much progress was achieved in incorporating effects of QCD evolution [29–33] which are taken into consideration approximately in our approach as described in Sec. 2.5 below. For the collinear pion distribution $f^a_{1,\pi}$, listed next in Fig. 2, many extractions are available [40–45]. We will use the MRSS fits [41].

One of the most prominent TMDs, the Sivers distribution $f^{\perp a}_{1T,p}$ was extracted from HERMES, COMPASS, and JLab SIDIS data by several groups with consistent results [34, 38, 86–94]. We will use the extractions of Ref. [34] labelled as "Torino" and Ref. [38] labelled as "JAM20".

The transversity distribution, $h^a_{1,p}$, plays a crucial role for understanding the nucleon spin structure. It is predicted to generate an asymmetry in SIDIS coupling to the Collins fragmentation function [95] which in turn is responsible for an asymmetry in e^+e^- into hadron pair production. We will use the "Torino" parametrizations of $h^a_{1,p}$ from a global QCD analysis of SIDIS and e^+e^- data [35] to be compared with model predictions, and the "JAM20" fit from a global QCD analysis of SIDIS, DY, e^+e^-, and proton-proton data [38] for comparisons and calculations.

The proton Boer-Mulders function, $h^{\perp a}_{1,p}$, was extracted from HERMES and COMPASS data and from DY measurements in Ref. [36] which we will use with the label "BMP10." The extraction of $h^{\perp a}_{1,p}$ [36] is less certain, because it is constrained by SIDIS data only, relies on the knowledge of the Collins function, and requires model-dependent corrections for sizable twist-4 power corrections (Cahn effect).

The so-called pretzelosity function $h^{\perp a}_{1T,p}$ was extracted in Ref. [37]. We will label $h^{\perp a}_{1T,p}$ from Ref. [37] as "LP15". Notice that large errors on extracted $h^{\perp a}_{1T,p}$ were reported in Ref. [37]. This is the least well known proton TMD for which an extraction has been attempted.

Only Kotzinian-Mulders distribution $h^{\perp a}_{1L,p}$ has not yet been extracted. It was found that the data related to this TMD are compatible with the WW-type approximation [39]. We will use this relation to approximate $h^{\perp a}_{1L,p}$ based on transversity $h^{\perp a}_{1,p}$ from [38].

Finally, the pion Boer-Mulders function $h^{\perp a}_{1,\pi}$ is the least known of the TMDs needed to describe pion-proton DY process at leading twist. No extractions are currently available for this TMD.

2.4 TMDs from models

In this section we briefly review the two CQM frameworks, the LFCQM and the SPM, and compare them to the available phenomenological extractions used in this work.

Light-front models are based on the decomposition of the hadron states in the Fock space constructed in the framework of light-front quantization. The hadron states are then obtained as a superposition of partonic quanta states, each one multiplied by a N-parton light-front wave function which gives the probability amplitude to finding the corresponding N-parton state in the hadron. In the LFCQM the light-front Fock expansion is truncated to the leading component given by the valence $3q$ and $q\bar{q}$ contribution in the proton and pion, respectively. The light-front wave functions can be further decomposed in terms of light-front wave amplitudes that are eigenstates of the total parton orbital angular momentum. The TMDs can then be expressed as overlap of light-front wave amplitudes with different orbital angular momentum [52] which makes very transparent the spin-orbit correlations encoded in the different TMDs [52, 53, 55–57]. To model the $3q$ light-front wave function of the proton, we use the phenomenological Ansatz of Ref. [96], describing the quark-momentum dependence through a rational analytical expression with parameters fitted to the anomalous magnetic moment of the proton and neutron [96, 97]. For the pion, we use the $q\bar{q}$ light-front wave function of Ref. [98], with the quark-momentum dependent part given by a Gaussian function with parameters fitted to the pion charge radius and decay constant.

Spectator models are based on a field theoretical description of deep inelastic scattering in a relativistic impulse approximation. In this parton model-like factorization the cross section for deep inelastic scattering processes can be expressed in terms of a Born cross section and quark correlation functions. In this framework, the quark correlation functions are hadronic matrix elements expanded in Dirac and flavor structure multiplying form factors. The essence of the SPMs is to calculate the matrix elements of the quark correlation function by the introduction of effective hadron-spectator-quark (e.g. nucleon-diquark-quark) vertices [47] which in turn enable one to model essential non-perturbative flavor and spin structure of hadrons.

The SPMs allow one to model the dynamics of universality and process dependence through studying the gauge-link, and phase content of TMDs [99–102]. In turn systematic phenomenological estimates for parton distributions and fragmentation functions for both "T-even" and "T-odd" TMDs have been carried out [48, 50, 103–107]. In regard to the latter, it is in this framework that the first calculations of the Sivers and Boer-Mulders functions of the nucleon were carried out [103–105] and shown on general grounds to contribute to semi-inclusive processes at leading power in the hard scale. Later the Boer-Mulders function of the pion was calculated in Ref. [49]. The model parameters are determined by comparing the SPM results for $f_{1,p}^u(x)$ and $f_{1,p}^d(x)$ to the leading order (LO) low-scale ($\mu_0^2 = 0.26$ GeV^2) data parametrization of Glück, Reya, and Vogt [25]. The proton TMDs for u- and d- quarks are given by linear combinations of contributions from axial vector and scalar diquarks assuming SU(2) flavor symmetry [47, 48].

The predictions from both models are shown along with the available parametrizations in Figs. 3-4 at a scale of 28 GeV^2. The (in some cases approximate) evolution is described in Sec. 2.4. The result from the LFCQM on $f_{1,\pi^-}^{\bar{u}}(x)$ (which coincides with $f_{1,\pi^-}^{d}(x)$ due to isospin symmetry) compares well to the MRSS parametrization [26], see Fig. 3. In the region $0.2 \lesssim x_\pi \lesssim 0.6$ which is relevant for COMPASS kinematics the SPM result agrees within 20-40 % with MRSS [26]. The two models agree well with each other in the case of the pion Boer-Mulders TMD $h_{1,\pi^-}^{\perp(1)\bar{u}}(x) = h_{1,\pi^-}^{\perp(1)d}(x)$ for which no extraction is available (so far). This robustness of the model predictions is important: the pion Boer-Mulders function enters 4 (out of 6) twist-2 pion-nucleon DY structure functions.

The results from the LFCQM and the SPM for the proton quark distributions are shown in Fig. 4. The region $0.05 \lesssim x \lesssim 0.3$ is probed in the COMPASS kinematics. The model results for the functions $f_{1,p}^u(x)$, $f_{1,p}^d(x)$, $f_{1T,p}^{(1)u}(x)$, $f_{1T,p}^{(1)d}(x)$, $h_{1,p}^d(x)$, $h_{1,p}^{\perp(1)d}(x)$, $h_{1L,p}^{(1)u}(x)$, $h_{1T,p}^{(2)u}(x)$ agree within 20-40 %, and for $h_{1,p}^u(x)$, $h_{1,p}^{\perp(1)u}(x)$, $h_{1L,p}^{(1)d}(x)$ within 40-60 %. Merely for $h_{1T,p}^{(2)d}(x)$ we observe a more sizable spread of model predictions. In all cases the models agree on the signs of the TMDs.

The model results for the unpolarized distributions agree reasonably well with MSTW [26]. The model predictions for transversity and Sivers function are compatible with the corresponding Torino [34, 35] and JAM20 fits [38]. The 1-σ uncertainty bands are shown for JAM20 [38]. The corresponding uncertainty bands of the Torino parametrizations [34, 35] are somewhat larger (as more data were used in the JAM20 analysis, cf. Sec. 2.3) and not displayed for better visibility. The proton Boer-Mulders function from models is in good agreement with the BMP10 extraction [36] which has significant statistical and systematic uncertainties, as discussed in Sec. 2.3, and are not

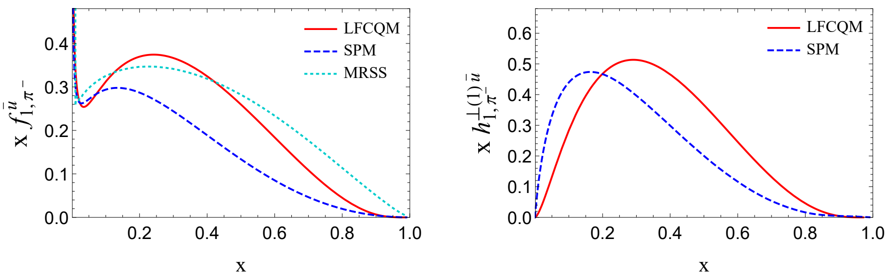

Figure 3. Left: $f_{1,\pi^-}^{\bar{u}}$ from LFCQM [57] and spectator model [49] LO-evolved to a scale of 28 GeV^2 in comparison to MRSS parametrization [41]. Right: Predictions from LFCQM [57] and SPM [49] for the pion Boer-Mulders function (with the sign for DY) for which no parametrizations are currently available.

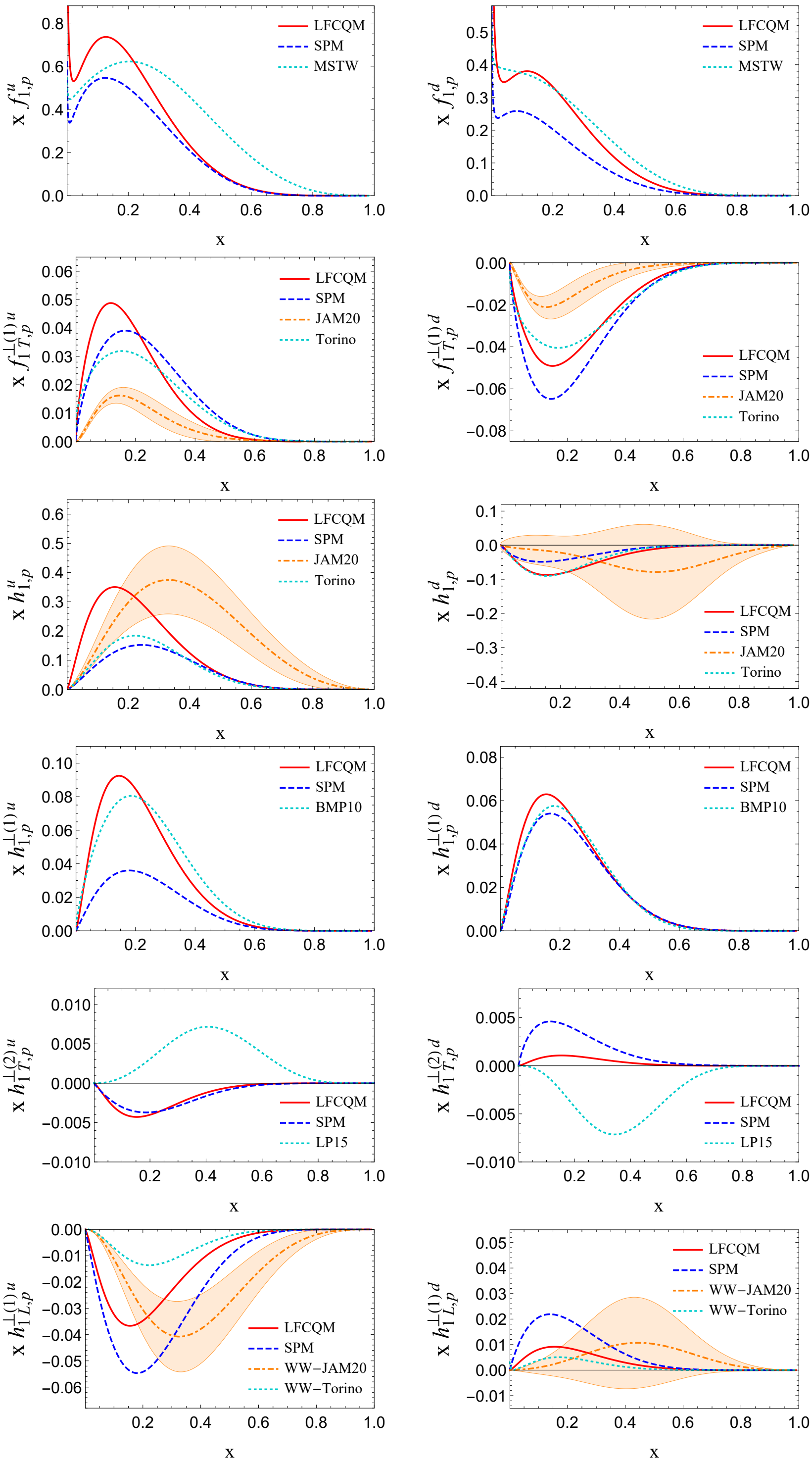

Figure 4. The proton TMDs of u and d quarks in LFCQM [52, 55, 56] and SPM [48] at a scale of 28 GeV^2 compared to phenomenological fits for $f_{1T,p}^{\perp(1)a}$ from JAM20 [38] and Torino [34], $h_{1,p}^{a}$ from JAM20 [38] and Torino [35], $h_{1,p}^{\perp(1)a}$ from BMP10 [36], $h_{1T,p}^{\perp(2)a}$ from LP15 [37]. Sivers and Boer-Mulders TMDs are shown with the sign for DY process. The error bands show the 1-σ uncertainty of the JAM20 extractions [38].

shown in Fig. 4. The model predictions for pretzelosity show little agreement with the best fit result from LP15 [37], but are within its 1-σ region which is not shown in the plot.

The comparison in Fig. 4 indicates an accuracy of the CQMs which is in many cases of the order of 20–40 %. Considering the much different physical foundations of the two models, one may speak about an overall robust CQM picture for the TMDs needed in our work.

2.5 Evolution of model results

TMDs computed in CQM framework refer to low initial scale $\mu_0 \simeq 450\,\text{MeV}$ [56, 57] and have to be evolved to experimentally relevant scales before they can be used for phenomenological applications. There are currently no exact methods to apply TMD evolution down to the very low model scales. The application of collinear DGLAP evolution down to such low scales is also subtle, but there is significant experience in this case: the familiar GRV parametrizations [23–25] have comparably low initial scales. We will utilize a pragmatic approach to account for evolution effects.

The evolution of TMDs is a double scale problem, and conveniently addressed in the impact parameter space with $\boldsymbol{b}_T$ the Fourier-conjugate variable to $\boldsymbol{k}_{Th}$. The TMDs in the impact parameter space are generically given by $f(x_h, \boldsymbol{b}_T, \mu, \zeta)$ where $\mu \sim Q$ is the "standard" renormalization scale for ultraviolet logarithms, and $\zeta \sim Q^2$ is the rapidity renormalization scale. In principle one can solve TMD evolution equations starting from some initial scale Q_0 without employing operator product expansion at low $\boldsymbol{b}_T$, see for instance Ref. [21]. The TMD at this scale is then $f(x_h, b_T, Q_0, Q_0^2)$. The unpolarized structure function is then very similar to parton model result, see Ref. [21],

$$F^1_{UU}(x_\pi, x_p, q_T, Q, Q^2) = \frac{1}{N_c}\sum_a e_a^2 \int \frac{b_T db_T}{2\pi} J_0(q_T b_T) \tilde{f}^a_{1,\pi}(x_\pi, b_T, Q_0, Q_0^2) \tilde{f}^{\bar{a}}_{1,p}(x_p, b_T, Q_0, Q_0^2) \times e^{-S(b_T, Q_0, Q_0^2, Q, Q^2)} \,, \tag{2.7}$$

where the factor $S(b, Q_0, Q_0^2, Q, Q^2)$ contains effects of gluon radiation with $S(b, Q_0, Q_0^2, Q_0, Q_0^2) = 0$ by construction. One can parametrize TMDs at initial scale Q_0 as:

$$\tilde{f}^a_{1,p}(x_h, \boldsymbol{b}_T, Q_0, Q_0^2) = f^a_{1,p}(x_h, Q_0)\; e^{-b_T^2 \frac{\langle k^2_{Th}\rangle_{f_{1,p}}}{4}} \,, \tag{2.8}$$

$$\tilde{f}^a_{1,\pi}(x_\pi, \boldsymbol{b}_T, Q_0, Q_0^2) = f^a_{1,\pi}(x_\pi, Q_0)\; e^{-b_T^2 \frac{\langle k^2_{T\pi}\rangle_{f_{1,\pi}}}{4}} \,, \tag{2.9}$$

which are the Fourier transformed expression for $f^a_{1,h}(x, \boldsymbol{k}_{Th})$ from Eq. (2.4) where $f^a_{1,p}(x_h, Q_0)$, $f^a_{1,\pi}(x_\pi, Q_0)$ are either phenomenological extractions or model calculations evolved to the scale Q_0 with collinear DGLAP evolution. The transverse momentum shape is parametrized as Gaussian with the values of the widths $\langle k^2_{Th}\rangle$, $\langle k^2_{T\pi}\rangle$ appropriate for the scale Q_0.

Expression of Eq. (2.7) is the result of TMD evolution using TMD factorization formalism as outlined in Ref. [21]. In order to do it in the full complexity, one needs to know details of the evolution kernel S in all values of b_T, which is currently under debate, see for instance Ref. [33]. We will choose instead the scale $Q_0 = 5.3$ GeV which corresponds to the mean value $\langle Q\rangle$ in the COMPASS experiment and use shapes from Eq. (2.4) directly in our computation. Notice that with this choice Eq. (2.7) will coincide with Eq. (2.6).

We use exact DGLAP evolution for $f^a_{1,h}(x)$ and $h^a_{1,p}(x)$. In all other cases we use approximate DGLAP evolution. For $f^{\perp(1)a}_{1T,p}(x)$ we use the $f^a_{1,h}(x)$-nonsinglet evolution shown to lead good results in the LFCQM model study of SIDIS asymmetries [56]. For all chiral-odd TMDs we assume the DGLAP evolution of transversity [55, 108].

The remaining problem is estimating the correct values for $\langle k^2_{Th}\rangle$ and $\langle k^2_{T\pi}\rangle$ at 5.3 GeV. The Gaussian model describes DY data well with Gaussian widths depending on the energy of the experiment: at higher energies, broader Gaussian distributions are needed, in qualitative agreement with CSS evolution [85]. At the initial scale in the LFCQM the k_T-distributions of the TMDs are approximately Gaussian with $\langle q_T^2\rangle_i = \langle k_{T\pi}^2\rangle_{f_{1,\pi}} + \langle k_{Tp}^2\rangle_{f_{1,p}} \approx 0.18\,\text{GeV}^2$ (this number weakly depends on x_π and x_p; the results are similar in the SPM). We estimate on the basis of [85] that at COMPASS energies $\langle q_T^2\rangle \approx 1.5\,\text{GeV}^2$ in the structure function F_{UU}^1, see [71] for comparison.

The study of [85] has been performed for the unpolarized DY process. At this point it is not known whether the Gaussian Ansatz works also for other structure functions. At low scales the LFCQM [56, 57] and many other models [64, 109, 110] support the Gaussian Ansatz approximately also for the Boer-Mulders and polarized TMDs, and we shall assume that it remains a useful approximation for these TMDs also at higher energies. Due to lack of data in these cases we have, however, no phenomenological guidance on the energy dependence of the Gaussian widths. It is natural to assume that also they are broadened with increasing energy though possibly to a lesser extent than in the case of unpolarized TMDs. In Ref. [57] the broadening was estimated for the structure function $F_{UU}^{\cos 2\phi}$ at beam energies somewhat higher than at COMPASS. On the basis of the results from [57] we estimate $\langle q_T^2\rangle \approx 1.2\,\text{GeV}^2$ at COMPASS for the structure function $F_{UU}^{\cos 2\phi}$. We estimate the k_T broadening of all structure functions involving chiral-odd TMDs to be approximately the same as for $F_{UU}^{\cos 2\phi}$. Finally, for $\langle q_T^2\rangle$ of $F_{UT}^{\sin\phi_S}$ it is natural to expect a value somewhere between the Gaussian widths of F_{UU}^1 and $F_{UU}^{\cos 2\phi}$, because here the broader width of an unpolarized TMD and a narrower width of a polarized TMD enter. We therefore assume $\langle q_T^2\rangle \approx 1.2\,\text{GeV}^2$ in this case.

To summarize, we perform the evolution of the model results with the Gaussian widths in (2.6) fixed as follows

$$\langle q_T^2\rangle \approx \begin{cases} 1.5\ \text{GeV}^2 & \text{for } F_{UU}^1, \\ 1.3\ \text{GeV}^2 & \text{for } F_{UT}^{\sin\phi_S}, \\ 1.2\ \text{GeV}^2 & \text{other cases.} \end{cases} \tag{2.10}$$

These estimates will be tested by experiments and phenomenological studies, and can be refined if needed.

3 Results and observations

In this section we briefly describe the COMPASS experiment, outline how we explore the model predictions and phenomenological TMD fits, present our results, and compare them to the data.

3.1 The COMPASS Drell-Yan experiment

The COMPASS 2015 data [46] were taken with a pion beam of 190 GeV impinging on a transversely polarized NH_3 target with a polarization of $\langle S_T\rangle = 73\,\%$ and a dilution factor $\langle f\rangle = 0.18$ [46]. The dimuon mass range 4.3 GeV $< Q^2 <$ 8.5 GeV above charmonium resonance region but below Υ threshold was covered with the mean value $\langle Q\rangle = 5.3\,\text{GeV}$. Due to the fixed target kinematics the pion structure was probed at higher $\langle x_\pi\rangle = 0.50$ compared to the proton $\langle x_p\rangle = 0.17$. The cut $q_T > 0.4\,\text{GeV}$ was imposed and $\langle q_T\rangle = 1.2\,\text{GeV}$ [46].

3.2 The approaches for numerical estimates

The Sivers asymmetry $A_{UT}^{\sin\phi}$ can be described completely in terms of both, model predictions and available parametrizations, and is the only asymmetry where the latter is possible. For the phenomenological calculation we will use the Torino [35] and JAM20 [38] analysis results for $f_{1T.p}^{\perp(1)a}(x)$, and MSTW [26] and MRSS [41] LO parametrizations for proton and pion unpolarized distributions.

The other asymmetries require the knowledge of the pion Boer-Mulders function for which no parametrization is available. In these cases we shall adopt two different main approaches, pure and hybrid, see Fig. 2 for an overview. We will present therefore up to four different calculations for each observable by exploring the model results and available parametrizations discussed in Sections 2.3, 2.4 and displayed in Figs. 3-4. The first approach makes a pure use of model predictions for all pion and proton TMDs which will be labelled in the plots by the acronyms LFCQM or SPM.

In the hybrid-approaches we will use the minimal model input, the predictions from the LFCQM and SPM for the pion Boer-Mulders function, and the maximal input from parametrizations: JAM20 [38] for $f_{1T,p}^{\perp a}$ and $h_{1,p}^{a}$, BMP10 [36] for $h_{1,p}^{\perp a}$, and LP15 [37] for $h_{1T,p}^{\perp a}$. The results will be labelled respectively as "LFC-JAM20", "LFC-LP15", "LFC-BMP10" or "SPM-JAM20," "SPM-LP15," "SPM-BMP10." For $h_{1L,p}^{\perp a}$ we make use of WW-type approximation which allows to approximate this TMD in terms of $h_{1,p}^{a}$ for which we will use JAM20 [38]. WW-type approximations were explored in Ref. [39] and shown to work well with the available data. We will add "WW" in the label of calculation when WW approximation is used. For all hybrid calculations we will use the parametrizations [26, 41] for $f_{1,p}^{a}$ and $f_{1,\pi}^{a}$

For our calculations we assume for the scale a value of $\langle Q\rangle^2 \approx 28\,\mathrm{GeV}^2$. The predictions from the models shown in Figs. 3-4 were evolved to this scale as described in Sec. 2.5. For the hybrid calculations we take into account k_T-broadening as discussed in Sec. 2.5.

3.3 Discussion of the results and comparison to available data

Numerical results for the leading-twist pion-nucleon DY asymmetries are shown in Figs. 5–9 in comparison to available COMPASS data. The Table 1 gives a detailed overview on the used model results and phenomenological information.

Let us start the discussion with $A_{UT}^{\sin\phi}$ asymmetry due to the Sivers function. One of the most striking features of "naively" T-odd (Sivers, Boer-Mulders) TMDs is the expected sign change [111] from SIDIS to DY due to the difference of initial (DY) vs final (SIDIS) state interactions [107, 112]. Verification of the sign change of the Sivers function is one of the milestones of DY programs of COMPASS and RHIC [113]. In SIDIS the proton u-quark Sivers function is negative, while in DY the STAR RHIC [114] $W^{\pm}/Z$ asymmetry data favor a positive sign [115]. This provides first experimental support for the predicted process dependence of T-odd TMDs [111].

The predictions for $A_{UT}^{\sin\phi}$ at COMPASS are positive, see for instance Refs. [116–118]. Our calculations confirm this expectation, see Fig. 5 where we compare our results to COMPASS data [46]. The u-quark Sivers function in DY is expected to be positive, see Fig. 4. If we disregard sea quark effects, which were shown to play a negligible role in π^--proton DY in the COMPASS kinematics [117], then $A_{UT}^{\sin\phi} \propto f_{1T,p}^{\perp u}(x_p) > 0$. The experimental error bars are currently sizeable, but the data show a tendency to positive asymmetry, see Fig. 5, in agreement with the expected sign change of the Sivers function. Clearly, more experimental evidence is needed to corroborate this finding.

In the global QCD analysis of single-spin asymmetries [38] the COMPASS data [46] were used, such that the JAM20 result in Fig. 5 is consistent with *all* present-day data on observables related to Sivers functions. It is worth remarking that predictions based on the earlier Torino extraction [34] (which used SIDIS data only) yield a somewhat larger asymmetry than JAM20 and are closer to the LFCQM and SPM results in Fig. 5. This result is consistent with the different size of Sivers functions found in Ref. [34] and Ref. [38], see Fig. 4.

Fig. 6 shows the asymmetry $A_{UT}^{\sin(2\phi-\phi_S)}$ which arises from a convolution of transversity and pion Boer-Mulders function in comparison to COMPASS data [46]. In the case of this asymmetry the pure model and hybrid calculations yield results in good mutual agreement. Neglecting sea quarks, it is $A_{UT}^{\sin(2\phi-\phi_S)} \propto -h_{1,\pi^-}^{\perp(1)\bar{u}}(x_\pi)h_{1,p}^{u}(x_p) < 0$. Both, $h_{1,\pi^-}^{\perp(1)\bar{u}}$ and $h_{1,p}^{u}$ are positive, see Fig 4, and we predict a negative asymmetry. This is consistent with the trend of the data. We therefore conclude that the COMPASS data [46] indicate a positive sign for the pion Boer-Mulders TMD $h_{1,\pi^-}^{\perp(1)\bar{u}}$. (It is important to recall that absolute signs in extractions of chiral-odd TMDs and fragmentation functions are convention-dependent because chiral-odd functions contribute to observables always in connection with other chiral-odd functions. The convention used for TMD

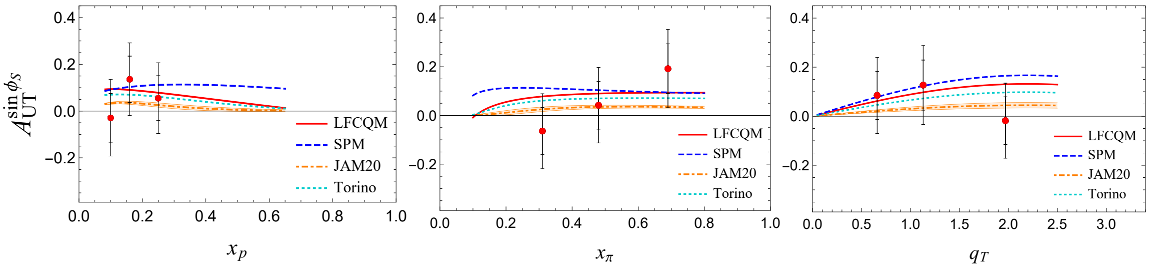

Figure 5. $A_{UT}^{\sin\phi}$ as a function of x_p (left), x_π (middle) and q_T (right) vs COMPASS data [46].

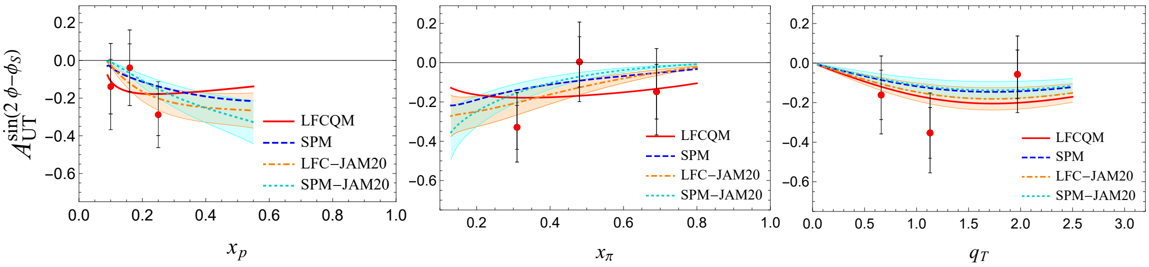

Figure 6. $A_{UT}^{\sin(2\phi-\phi_S)}$ as a function of x_p (left), x_π (middle) and q_T (right) vs COMPASS data [46].

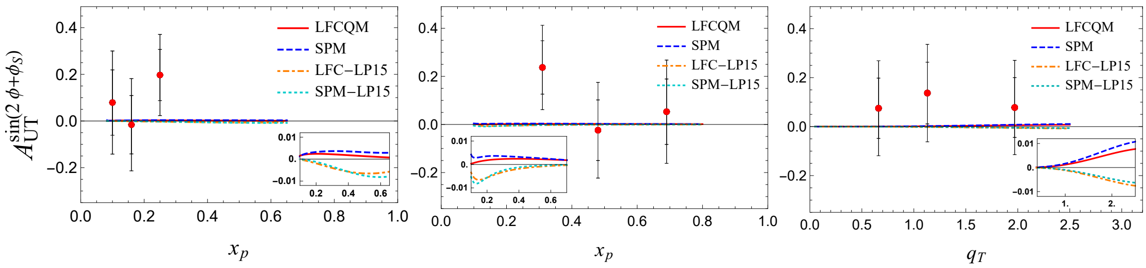

Figure 7. $A_{UT}^{\sin(2\phi+\phi_S)}$ as a function of x_p (left), x_π (middle) and q_T (right) vs COMPASS data [46].

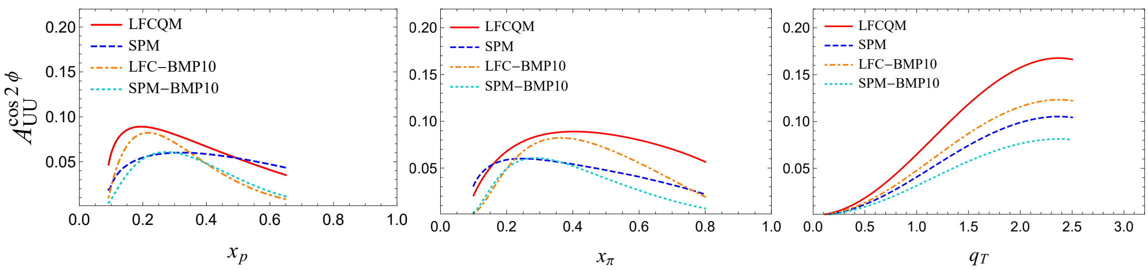

Figure 8. $A_{UU}^{\cos 2\phi}$ as a function of x_p (left), x_π (middle) and q_T (right) in the COMPASS kinematics.

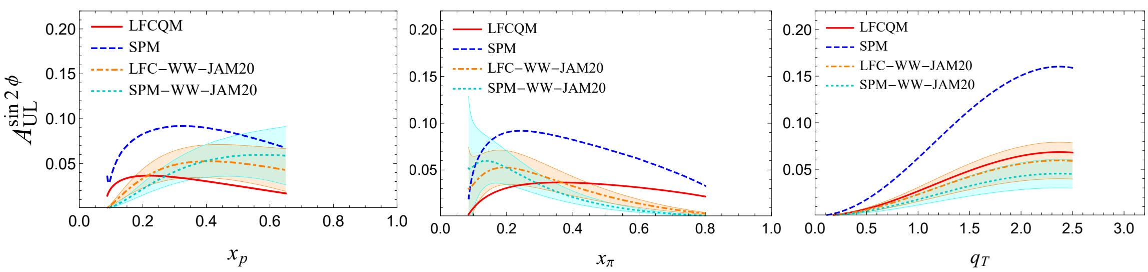

Figure 9. $A_{UL}^{\sin 2\phi}$ as a function of x_p (left), x_π (middle) and q_T (right) in the COMPASS kinematics.

extractions is $h^u_{1,p}(x) > 0$. This sign is a choice which is well-informed by model and lattice QCD calculations but not an experimental observation.) The indication that $h^{\perp(1)\bar{u}}_{1,\pi^-} > 0$ is an important result which can be used to test the process dependence of the proton Boer-Mulders function, see below.

Fig. 7 shows $A_{UT}^{\sin(2\phi+\phi_S)}$ which is due the convolution of pretzelosity and pion Boer-Mulders function compared to COMPASS data [46]. This asymmetry is proportional to q_T^3 for $q_T \ll 1\,\mathrm{GeV}$. This leads to a kinematic suppression of this asymmetry as compared to the two previous asymmetries (both proportional to q_T at small transverse momenta). As a consequence $A_{UT}^{\sin(2\phi+\phi_S)}$ is by far the smallest of the leading-twist asymmetries in pion-nucleon DY. Numerically it is 1 % or smaller, such that we had to include the insets in Fig. 7 to display the theoretical curves. The LFCQM and the SPM are in good agreement with each other, but not with the LP15 fit of pretzelosity [37] which suggests an opposite sign for the asymmetry. At this point one has to stress that the LP15 fit of [37] has a large statistical uncertainty (not displayed in Figs. 4 and 7) and is compatible with zero or opposite sign within 1-σ. This TMD is difficult to measure in DY and SIDIS. In the high luminosity SIDIS experiments at JLab 12 GeV and the future Electron Ion Collider it may be feasible to measure pretzelosity.

The $A_{UU}^{\cos 2\phi}$ asymmetry in unpolarized DY originates from a convolution of the Boer-Mulders functions in nucleon and pion. Historically it was connected to the "violation" of the Lam-Tung relation, see [119] and references therein. A simultaneous measurement of $A_{UU}^{\cos 2\phi}$ and $A_{UT}^{\sin(2\phi-\phi_S)}$ which we have discussed above allows one to test the sign change of the proton Boer-Mulders function in DY. $A_{UU}^{\cos 2\phi}$ was measured and found positive in earlier CERN and Fermilab measurements [120, 121]. Neglecting sea quark effects, the asymmetry is dominated by $A_{UU}^{\cos 2\phi} \propto h^{\perp(1)\bar{u}}_{1,\pi^-}(x_\pi) h^{\perp(1)u}_{1,p}(x_p)$. With the indication of the positive sign for the pion Boer-Mulders function from the COMPASS data [46] on $A_{UT}^{\sin(2\phi-\phi_S)}$, we conclude a positive sign also for the proton u-quark Boer-Mulders function in DY, which is opposite to the sign seen in SIDIS analyses [122] and hence in agreement with the prediction for the process dependence property of T-odd TMDs [111].

Fig. 8 shows our predictions for $A_{UU}^{\cos 2\phi}$ for COMPASS kinematics. At this point no data are available from COMPASS, but an analysis is under way [123] and our predictions in Fig. 8 will be tested in near future. It is worth recalling that our approach provides a good description of the NA10 CERN [120] and E615 Fermilab [121] data. The test of our predictions in Fig. 8 will help to investigate the compatibility of the NA10, E615 and COMPASS experiments. Interestingly, fixed-order collinear factorized perturbative QCD calculations, which strictly speaking require q_T to be the hard scale, can also qualitatively describe the NA10 and E615 data [67, 68]. It will be interesting to confront those calculations with future COMPASS data and TMD studies.

Notice that in the analysis [122] of the proton-proton and proton-deuteron data from the FNAL E866/NuSea experiment [124, 125] indications were obtained that the proton quark and antiquark Boer-Mulders functions (in DY) have the same signs. With our observations based on COMPASS data we therefore infer a first hint that also the Boer-Mulders functions of $\bar{u}$ and $\bar{d}$ are positive in DY. Interestingly, not only valence Boer-Mulders distributions in nucleon and pion seem "alike" [126], but also the nucleon sea quark distributions seem to have all the same sign. This in line with predictions from the limit of a large number of colors N_c in QCD that $h^{\perp u}_{1,p}(x_p, \boldsymbol{k}_{Tp}) = h^{\perp d}_{1,p}(x_p, \boldsymbol{k}_{Tp})$ and $h^{\perp \bar{u}}_{1,p}(x_p, \boldsymbol{k}_{Tp}) = h^{\perp \bar{d}}_{1,p}(x_p, \boldsymbol{k}_{Tp})$ modulo $1/N_c$ corrections [127]. Future data will provide more stringent tests of these predictions.

Finally it is worth recalling that in principle one can extract the u-quark transversity distribution entirely from the measurements of $A_{UU}^{\cos 2\phi}$ and $A_{UT}^{\sin(2\phi-\phi_S)}$ in π^--proton DY at COMPASS [128]. While typically data available from different processes are processed in "global analyses," whenever possible it is also valuable to extract a function from one process alone. This would for instance allow one to test the universality (same sign and x-shape in SIDIS and DY) of the u-quark

Fig.	structure function	TMDs	LFCQM	SPM	phenomenology
5-9	F_{UU}	$f^a_{1,p}$, $f^a_{1,\pi}$	[52], [57]	[48] [49]	[26], [41]
5	$F^{\sin\phi}_{UT}$	$f^{\perp a}_{1T,p}$, $f^a_{1,\pi}$	[53], [57]	[48], [49]	[38], [41]
6	$F^{\sin(2\phi-\phi_S)}_{UT}$	$h^a_{1,p}$, $h^{\perp a}_{1,\pi}$	[52], [57]	[48], [49]	[38], —
7	$F^{\sin(2\phi+\phi_S)}_{UT}$	$h^{\perp a}_{1T,p}$, $h^{\perp a}_{1,\pi}$	[52], [57]	[47], [49]	[37], —
8	$F^{\cos 2\phi}_{UU}$	$h^{\perp a}_{1,p}$, $h^{\perp a}_{1,\pi}$	[53], [57]	[48], [49]	[36], —
9	$F^{\sin 2\phi}_{UL}$	$h^{\perp a}_{1L,p}$, $h^{\perp a}_{1,\pi}$	[52], [57]	[48], [49]	[39], —

Table 1. Overview on non-perturbative input used to produce the result in Figs. 5–9 which was taken from the LFCQM, the SPM, and phenomenological fits (or WW-type approximation in the case of $h^{\perp a}_{1L,p}$). Notice that no phenomenological information is currently available on $h^{\perp a}_{1,\pi}$, cf. Sec. 2.3. .

transversity distribution which is otherwise taken for granted.

Fig. 9 displays our predictions for the longitudinal single-spin asymmetry $A^{\sin 2\phi}_{UL}$ in the COMPASS kinematics which is due to the Kotzinian-Mulders TMD $h^{\perp a}_{1L}$ and the pion Boer-Mulders function. If we disregard sea quark effects, then $A^{\sin 2\phi}_{UL} \propto -h^{\perp(1)\bar{u}}_{1,\pi^-}(x_\pi)h^{\perp(1)u}_{1L,p}(x_p) > 0$. Especially the SPM predicts a sizable and positive asymmetry. Since no parametrization on $h^{\perp a}_{1L}$ is currently available, the hybrid calculations make use of the WW-type approximation which is compatible with SIDIS data [39]. This is the only leading-twist pion-proton asymmetry in DY which requires a longitudinal proton polarization. We are not aware of plans to run the pion-nucleon DY experiment at COMPASS with a longitudinally polarized target in the near future. Our results in Fig. 9 therefore constitute predictions that may be awaiting experimental tests in the more distant future.

4 Conclusions

In this work we studied the DY process with negative pions and polarized protons with focus on the kinematics of the COMPASS experiment. As no phenomenological extractions are available for one of the involved TMDs, the Boer-Mulders function of the pion, we explored two popular and widely used hadronic models, the LFCQM and SPM, together with available phenomenological information on the other TMDs.

We presented a complete description of polarized DY at leading twist. This requires on the nucleon side $f^a_{1,p}$, $f^{\perp a}_{1T,p}$, $h^a_{1,p}$, $h^{\perp a}_{1,p}$, $h^{\perp a}_{1T,p}$, $h^{\perp a}_{1L,p}$; and on the pion side $f^a_{1,\pi}$, $h^{\perp a}_{1,\pi}$. For that we compiled results from several prior LFCQM and SPM calculations, which to the best of our knowledge have not been presented in this completeness before [47–49, 52, 53, 57]. Based on concise comparisons of model results with available phenomenological information [26, 34–39, 41], we estimate an accuracy of the model results of 20-40 % for the majority of (though not all) TMDs. Similar "model accuracies" were found in prior phenomenological applications of CQMs [55–57]. The model results were evolved from their low initial scales $\mu_0 < 1\,\text{GeV}$ to the scale of the COMPASS experiment $\langle Q \rangle = 5.3\,\text{GeV}$ by means of an approximate evolution which was tested in prior applications of CQMs to the description of SIDIS and DY data.

Driven by the motivation to make maximal use of currently available phenomenological information [26, 34–39, 41], we made also "hybrid" calculations with a minimal model dependence — namely only due to the pion Boer-Mulders function for which no extraction is currently available. In this way we provided up to four complementary predictions for each DY observable, with different levels of model dependence. The critical comparison of the different results (pure-model and hybrid calculations in respectively LFCQM and SPM) allows us to differentiate robust predictions from more strongly model-dependent results.

Our study had two main goals, namely to present theoretical calculations which help to interpret the first data from the pion-induced DY with polarized protons measured by COMPASS, as well as to prepare quantitative tests of the application of CQMs to the description of pion and nucleon structure.

In regard to the interpretation of the first data from the pion-induced DY with polarized protons, we observe a robust picture. The pure-model and hybrid calculations from the LFCQM and SPM are in remarkable agreement with each other at the present stage. The theoretical spread of our results is smaller than the present uncertainties of the available data. Among the most interesting observations are the encouraging indications for the change of sign of the T-odd TMDs in DY vs SIDIS, both in the case of the proton Sivers and proton Boer-Mulders function. These are model independent results. Another model-independent result is the observation that the data favor a positive (in DY) Boer-Mulders $\bar{u}$-distribution in π^-. We also report the first indication that all proton Boer-Mulders functions for u, d, $\bar{u}$, $\bar{d}$ flavors are positive (in DY). At the present, these observations are admittedly vague due to the insufficient precision of the available experimental data. More precise future data from COMPASS and other facilities will allow us to solidify the picture.

In regard to the quantitative tests of the application of CQMs, it is important to stress that the DY process with π^- and proton in the COMPASS kinematics is an ideal process for these purposes. In the COMPASS kinematics sea quarks do not play an important role [117]. Due to the u-quark dominance in the proton the process is strongly dominated by annihilations of valence-$\bar{u}$ at $\langle x_\pi \rangle = 0.50$ from π^- and valence-u at $\langle x_p \rangle = 0.17$ from proton. These are the x-ranges where CQMs can be expected to catch the main features in the hadronic structure of the pion and nucleon. Our results are compatible with the data, though one also has to admit that the experimental uncertainties are currently still large.

CQMs are important qualitative tools for QCD calculations. Within their model accuracy of 20-40 % and within their range of applicability which is in the valence x-region, we observe that CQMs yield useful results and provide helpful guidelines for the interpretation of data. Future data will provide more stringent tests of the CQMs, and allow for extraction of hadron structure by global QCD analyses.

We provided several predictions that await experimental confirmation. Among those at least the $A_{UU}^{\cos(2\phi)}$ measurements are expected to come soon [123] and will become a stringent test of our findings.

Acknowledgments

The authors wish to thank A. V. Efremov for valuable discussions which motivated this study. This work was supported by the National Science Foundation under the Contracts No. PHY-1812423 (S.B. and P.S.) and No. PHY-1623454 (A.P.), the DOE Contracts No. DE-AC05-06OR23177 (L.G.) and No. DE-AC05-06OR23177 (A.P.) under which JSA, LLC operates JLab, the framework of the TMD Topical Collaboration, and by the European Union's Horizon 2020 programme under grant agreement No. 824093(STRONG2020) (B.P.).

References

[1] J. C. Collins, D. E. Soper and G. Sterman, *Transverse Momentum Distribution in Drell–Yan Pair and W and Z Boson Production*, *Nucl. Phys.* **B250** (1985) 199.

[2] J. Collins, *Foundations of perturbative QCD*, vol. 32. Cambridge University Press, 11, 2013.

[3] R. N. Cahn, *Azimuthal Dependence in Leptoproduction: A Simple Parton Model Calculation*, *Phys. Lett.* **B78** (1978) 269.

[4] D. W. Sivers, *Single spin production asymmetries from the hard scattering of point-like constituents*, *Phys. Rev.* **D41** (1990) 83.

[5] M. Anselmino, M. Boglione and F. Murgia, *Single spin asymmetry for p (polarized) $p \to \pi X$ in perturbative QCD*, *Phys. Lett.* **B362** (1995) 164–172, [hep-ph/9503290].

[6] A. Kotzinian, *New quark distributions and semiinclusive electroproduction on the polarized nucleons*, *Nucl. Phys.* **B441** (1995) 234–248, [hep-ph/9412283].

[7] P. J. Mulders and R. D. Tangerman, *The complete tree-level result up to order 1/Q for polarized deep-inelastic leptoproduction*, *Nucl. Phys.* **B461** (1996) 197–237, [hep-ph/9510301].

[8] A. M. Kotzinian and P. J. Mulders, *Longitudinal quark polarization in transversely polarized nucleons*, *Phys. Rev.* **D54** (1996) 1229–1232, [hep-ph/9511420].

[9] A. Bacchetta et al., *Semi-inclusive deep inelastic scattering at small transverse momentum*, *JHEP* **02** (2007) 093, [hep-ph/0611265].

[10] R. Tangerman and P. J. Mulders, *Intrinsic transverse momentum and the polarized Drell-Yan process*, *Phys. Rev. D* **51** (1995) 3357–3372, [hep-ph/9403227].

[11] D. Boer and P. J. Mulders, *Time-reversal odd distribution functions in leptoproduction*, *Phys. Rev.* **D57** (1998) 5780–5786, [hep-ph/9711485].

[12] S. Arnold, A. Metz and M. Schlegel, *Dilepton production from polarized hadron hadron collisions*, *Phys. Rev.* **D79** (2009) 034005, [0809.2262].

[13] A. Metz and A. Vossen, *Parton Fragmentation Functions*, *Prog. Part. Nucl. Phys.* **91** (2016) 136–202, [1607.02521].

[14] J. C. Collins and D. E. Soper, *Back-To-Back Jets in QCD*, *Nucl. Phys.* **B193** (1981) 381.

[15] J.-w. Qiu and G. F. Sterman, *Single transverse spin asymmetries*, *Phys. Rev. Lett.* **67** (1991) 2264–2267.

[16] X. Ji, J.-p. Ma and F. Yuan, *QCD factorization for semi-inclusive deep-inelastic scattering at low transverse momentum*, *Phys. Rev.* **D71** (2005) 034005, [hep-ph/0404183].

[17] X. Ji, J.-W. Qiu, W. Vogelsang and F. Yuan, *Single-transverse spin asymmetry in semi-inclusive deep inelastic scattering*, *Phys. Lett.* **B638** (2006) 178–186, [hep-ph/0604128].

[18] X. Ji, J.-W. Qiu, W. Vogelsang and F. Yuan, *Single transverse-spin asymmetry in Drell-Yan production at large and moderate transverse momentum*, *Phys. Rev.* **D73** (2006) 094017, [hep-ph/0604023].

[19] S. M. Aybat, A. Prokudin and T. C. Rogers, *Calculation of TMD Evolution for Transverse Single Spin Asymmetry Measurements*, *Phys. Rev. Lett.* **108** (2012) 242003, [1112.4423].

[20] J. P. Ma and G. P. Zhang, *QCD Corrections of All Structure Functions in Transverse Momentum Dependent Factorization for Drell-Yan Processes*, *JHEP* **02** (2014) 100, [1308.2044].

[21] J. Collins and T. Rogers, *Understanding the large-distance behavior of transverse-momentum-dependent parton densities and the Collins-Soper evolution kernel*, *Phys. Rev. D* **91** (2015) 074020, [1412.3820].

[22] J. Collins, L. Gamberg, A. Prokudin, T. C. Rogers, N. Sato and B. Wang, *Relating Transverse Momentum Dependent and Collinear Factorization Theorems in a Generalized Formalism*, *Phys. Rev.* **D94** (2016) 034014, [1605.00671].

[23] M. Gluck, E. Reya and A. Vogt, *Parton distributions for high-energy collisions*, *Z. Phys.* **C53** (1992) 127–134.

[24] M. Gluck, E. Reya and A. Vogt, *Dynamical parton distributions of the proton and small x physics*, *Z. Phys.* **C67** (1995) 433–448.

[25] M. Gluck, E. Reya and A. Vogt, *Dynamical parton distributions revisited*, *Eur. Phys. J.* **C5** (1998) 461–470, [hep-ph/9806404].

[26] A. D. Martin, W. J. Stirling, R. S. Thorne and G. Watt, *Parton distributions for the LHC*, *Eur. Phys. J.* **C63** (2009) 189–285, [0901.0002].

[27] L. Harland-Lang, A. Martin, P. Motylinski and R. Thorne, *Parton distributions in the LHC era: MMHT 2014 PDFs*, *Eur. Phys. J. C* **75** (2015) 204, [1412.3989].

[28] S. Dulat, T.-J. Hou, J. Gao, M. Guzzi, J. Huston, P. Nadolsky et al., *New parton distribution functions from a global analysis of quantum chromodynamics*, *Phys. Rev. D* **93** (2016) 033006, [1506.07443].

[29] F. Landry, R. Brock, P. M. Nadolsky and C. Yuan, *Tevatron Run-1 Z boson data and Collins-Soper-Sterman resummation formalism*, *Phys. Rev. D* **67** (2003) 073016, [hep-ph/0212159].

[30] M. Anselmino, M. Boglione, J. Gonzalez Hernandez, S. Melis and A. Prokudin, *Unpolarised Transverse Momentum Dependent Distribution and Fragmentation Functions from SIDIS Multiplicities*, *JHEP* **04** (2014) 005, [1312.6261].

[31] A. Signori, A. Bacchetta, M. Radici and G. Schnell, *Investigations into the flavor dependence of partonic transverse momentum*, *JHEP* **11** (2013) 194, [1309.3507].

[32] A. Bacchetta, V. Bertone, C. Bissolotti, G. Bozzi, F. Delcarro, F. Piacenza et al., *Transverse-momentum-dependent parton distributions up to N^3LL from Drell-Yan data*, 1912.07550.

[33] I. Scimemi and A. Vladimirov, *Non-perturbative structure of semi-inclusive deep-inelastic and Drell-Yan scattering at small transverse momentum*, 1912.06532.

[34] M. Anselmino, M. Boglione, U. D'Alesio, S. Melis, F. Murgia and A. Prokudin, *Sivers Distribution Functions and the Latest SIDIS Data*, in *19th International Workshop on Deep-Inelastic Scattering and Related Subjects (DIS 2011) Newport News, Virginia, April 11-15, 2011*, 2011. 1107.4446.

[35] M. Anselmino, M. Boglione, U. D'Alesio, S. Melis, F. Murgia and A. Prokudin, *Simultaneous extraction of transversity and Collins functions from new SIDIS and e+e- data*, *Phys. Rev.* **D87** (2013) 094019, [1303.3822].

[36] V. Barone, S. Melis and A. Prokudin, *The Boer-Mulders effect in unpolarized SIDIS: An Analysis of the COMPASS and HERMES data on the cos 2 phi asymmetry*, *Phys. Rev.* **D81** (2010) 114026, [0912.5194].

[37] C. Lefky and A. Prokudin, *Extraction of the distribution function $h_{1T}^{\perp}$ from experimental data*, *Phys. Rev.* **D91** (2015) 034010, [1411.0580].

[38] J. Cammarota, L. Gamberg, Z.-B. Kang, J. A. Miller, D. Pitonyak, A. Prokudin et al., *The origin of single transverse-spin asymmetries in high-energy collisions*, 2002.08384.

[39] S. Bastami et al., *Semi-Inclusive Deep Inelastic Scattering in Wandzura-Wilczek-type approximation*, *JHEP* **06** (2019) 007, [1807.10606].

[40] M. Glück, E. Reya and A. Vogt, *Pionic parton distributions*, *Z. Phys. C* **53** (1992) 651–656.

[41] P. J. Sutton, A. D. Martin, R. G. Roberts and W. J. Stirling, *Parton distributions for the pion extracted from Drell-Yan and prompt photon experiments*, *Phys. Rev.* **D45** (1992) 2349–2359.

[42] M. Glück, E. Reya and I. Schienbein, *Pionic parton distributions revisited*, *Eur. Phys. J. C* **10** (1999) 313–317, [hep-ph/9903288].

[43] M. Aicher, A. Schafer and W. Vogelsang, *Soft-gluon resummation and the valence parton distribution function of the pion*, *Phys. Rev. Lett.* **105** (2010) 252003, [1009.2481].

[44] P. Barry, N. Sato, W. Melnitchouk and C.-R. Ji, *First Monte Carlo Global QCD Analysis of Pion Parton Distributions*, *Phys. Rev. Lett.* **121** (2018) 152001, [1804.01965].

[45] I. Novikov et al., *Parton Distribution Functions of the Charged Pion Within The xFitter Framework*, 2002.02902.

[46] COMPASS collaboration, M. Aghasyan et al., *First measurement of transverse-spin-dependent azimuthal asymmetries in the Drell-Yan process*, *Phys. Rev. Lett.* **119** (2017) 112002, [1704.00488].

[47] R. Jakob, P. Mulders and J. Rodrigues, *Modeling quark distribution and fragmentation functions*, *Nucl. Phys. A* **626** (1997) 937–965, [hep-ph/9704335].

[48] L. P. Gamberg, G. R. Goldstein and M. Schlegel, *Transverse Quark Spin Effects and the Flavor Dependence of the Boer-Mulders Function*, *Phys. Rev.* **D77** (2008) 094016, [0708.0324].

[49] L. Gamberg and M. Schlegel, *Final state interactions and the transverse structure of the pion using non-perturbative eikonal methods*, *Phys. Lett. B* **685** (2010) 95–103, [0911.1964].

[50] A. Bacchetta, F. Conti and M. Radici, *Transverse-momentum distributions in a diquark spectator model*, *Phys. Rev. D* **78** (2008) 074010, [0807.0323].

[51] Z. Lu and B.-Q. Ma, *Non-zero transversity distribution of the pion in a quark-spectator-antiquark model*, *Phys. Rev. D* **70** (2004) 094044, [hep-ph/0411043].

[52] B. Pasquini, S. Cazzaniga and S. Boffi, *Transverse momentum dependent parton distributions in a light-cone quark model*, *Phys. Rev.* **D78** (2008) 034025, [0806.2298].

[53] B. Pasquini and F. Yuan, *Sivers and Boer-Mulders functions in Light-Cone Quark Models*, *Phys. Rev. D* **81** (2010) 114013, [1001.5398].

[54] C. Lorcé, B. Pasquini and M. Vanderhaeghen, *Unified framework for generalized and transverse-momentum dependent parton distributions within a 3Q light-cone picture of the nucleon*, *JHEP* **05** (2011) 041, [1102.4704].

[55] S. Boffi, A. V. Efremov, B. Pasquini and P. Schweitzer, *Azimuthal spin asymmetries in light-cone constituent quark models*, *Phys. Rev.* **D79** (2009) 094012, [0903.1271].

[56] B. Pasquini and P. Schweitzer, *Naive time-reversal odd phenomena in semi-inclusive deep-inelastic scattering from light-cone constituent quark models*, *Phys. Rev.* **D83** (2011) 114044, [1103.5977].

[57] B. Pasquini and P. Schweitzer, *Pion transverse momentum dependent parton distributions in a light-front constituent approach, and the Boer-Mulders effect in the pion-induced Drell-Yan process*, *Phys. Rev.* **D90** (2014) 014050, [1406.2056].

[58] C. Lorcé, B. Pasquini and P. Schweitzer, *Unpolarized transverse momentum dependent parton distribution functions beyond leading twist in quark models*, *JHEP* **01** (2015) 103, [1411.2550].

[59] C. Lorcé, B. Pasquini and P. Schweitzer, *Transverse pion structure beyond leading twist in constituent models*, *Eur. Phys. J. C* **76** (2016) 415, [1605.00815].

[60] F. Yuan, *Sivers function in the MIT bag model*, *Phys. Lett. B* **575** (2003) 45–54, [hep-ph/0308157].

[61] H. Avakian, A. Efremov, P. Schweitzer and F. Yuan, *Transverse momentum dependent distribution function $h_{1T}^{\perp}$ the single spin asymmetry $A_{UT}^{\sin(3\phi-\phi_S)}$*, *Phys. Rev. D* **78** (2008) 114024, [0805.3355].

[62] A. Courtoy, F. Fratini, S. Scopetta and V. Vento, *A Quark model analysis of the Sivers function*, *Phys. Rev. D* **78** (2008) 034002, [0801.4347].

[63] A. Courtoy, S. Scopetta and V. Vento, *Model calculations of the Sivers function satisfying the Burkardt Sum Rule*, *Phys. Rev. D* **79** (2009) 074001, [0811.1191].

[64] H. Avakian, A. V. Efremov, P. Schweitzer and F. Yuan, *The transverse momentum dependent distribution functions in the bag model*, *Phys. Rev.* **D81** (2010) 074035, [1001.5467].

[65] S. Noguera and S. Scopetta, *Pion transverse momentum dependent parton distributions in the Nambu and Jona-Lasinio model*, *JHEP* **11** (2015) 102, [1508.01061].

[66] M. Engelhardt, P. Hägler, B. Musch, J. Negee and A. Schäfer, *Lattice QCD study of the Boer-Mulders effect in a pion*, *Phys. Rev. D* **93** (2016) 054501, [1506.07826].

[67] M. Lambertsen and W. Vogelsang, *Drell-Yan lepton angular distributions in perturbative QCD*, *Phys. Rev. D* **93** (2016) 114013, [1605.02625].

[68] W.-C. Chang, R. E. McClellan, J.-C. Peng and O. Teryaev, *Lepton Angular Distributions of Fixed-target Drell-Yan Experiments in Perturbative QCD and a Geometric Approach*, *Phys. Rev. D* **99** (2019) 014032, [1811.03256].

[69] A. Bacchetta, S. Cotogno and B. Pasquini, *The transverse structure of the pion in momentum space inspired by the AdS/QCD correspondence*, *Phys. Lett. B* **771** (2017) 546–552, [1703.07669].

[70] W. Broniowski and E. Ruiz Arriola, *Partonic quasidistributions of the proton and pion from transverse-momentum distributions*, *Phys. Rev. D* **97** (2018) 034031, [1711.03377].

[71] F. A. Ceccopieri, A. Courtoy, S. Noguera and S. Scopetta, *Pion nucleus Drell–Yan process and parton transverse momentum in the pion*, *Eur. Phys. J. C* **78** (2018) 644, [1801.07682].

[72] X. Wang, Z. Lu and I. Schmidt, *Transverse momentum spectrum of dilepton pair in the unpolarized $\pi^- N$ Drell-Yan process within TMD factorization*, *JHEP* **08** (2017) 137, [1707.05207].

[73] A. Vladimirov, *Pion-induced Drell-Yan processes within TMD factorization*, *JHEP* **10** (2019) 090, [1907.10356].

[74] H. Li, X. Wang and Z. Lu, $\sin(2\phi - \phi_S)$ *azimuthal asymmetry in the pion induced Drell-Yan process within TMD factorization*, *Phys. Rev. D* **101** (2020) 054013, [1907.07095].

[75] X. Wang, W. Mao and Z. Lu, *Boer-Mulders effect in the unpolarized pion induced Drell–Yan process at COMPASS within TMD factorization*, *Eur. Phys. J. C* **78** (2018) 643, [1805.03017].

[76] X. Wang and Z. Lu, *Sivers asymmetry in the pion induced Drell-Yan process at COMPASS within transverse momentum dependent factorization*, *Phys. Rev. D* **97** (2018) 054005, [1801.00660].

[77] P. Ratcliffe, *Radiative Corrections to the Helicity Asymmetries for the Drell-Yan Process in QCD*, *Nucl. Phys. B* **223** (1983) 45–60.

[78] A. Weber, *Soft gluon resummations for polarized Drell-Yan dimuon production*, *Nucl. Phys. B* **382** (1992) 63–96.

[79] W. Vogelsang and A. Weber, *Drell-Yan dimuon production with transversely polarized protons*, *Phys. Rev. D* **48** (1993) 2073–2082.

[80] A. Contogouris, B. Kamal and Z. Merebashvili, *One loop corrections to lepton pair production by transversely polarized hadrons*, *Phys. Lett. B* **337** (1994) 169–175.

[81] T. Gehrmann, *QCD corrections to the longitudinally polarized Drell-Yan process*, *Nucl. Phys. B* **498** (1997) 245–266, [hep-ph/9702263].

[82] G. Bunce, N. Saito, J. Soffer and W. Vogelsang, *Prospects for spin physics at RHIC*, *Ann. Rev. Nucl. Part. Sci.* **50** (2000) 525–575, [hep-ph/0007218].

[83] H. Shimizu, G. F. Sterman, W. Vogelsang and H. Yokoya, *Dilepton production near partonic threshold in transversely polarized proton-antiproton collisions*, *Phys. Rev. D* **71** (2005) 114007, [hep-ph/0503270].

[84] U. D'Alesio and F. Murgia, *Parton intrinsic motion in inclusive particle production: Unpolarized cross sections, single spin asymmetries and the Sivers effect*, *Phys. Rev.* **D70** (2004) 074009, [hep-ph/0408092].

[85] P. Schweitzer, T. Teckentrup and A. Metz, *Intrinsic transverse parton momenta in deeply inelastic reactions*, *Phys. Rev.* **D81** (2010) 094019, [1003.2190].

[86] M. Anselmino, M. Boglione, U. D'Alesio, S. Melis, F. Murgia and A. Prokudin, *New insight on the Sivers transverse momentum dependent distribution function*, *J. Phys. Conf. Ser.* **295** (2011) 012062, [1012.3565].

[87] M. Anselmino, M. Boglione, U. D'Alesio, A. Kotzinian, F. Murgia and A. Prokudin, *Extracting the Sivers function from polarized SIDIS data and making predictions*, *Phys. Rev. D* **72** (2005) 094007, [hep-ph/0507181].

[88] M. Anselmino et al., *Comparing extractions of Sivers functions*, in *International Workshop on Transverse Polarization Phenomena in Hard Processes*, pp. 236–243, 11, 2005. hep-ph/0511017. DOI.

[89] J. Collins, A. Efremov, K. Goeke, S. Menzel, A. Metz and P. Schweitzer, *Sivers effect in semi-inclusive deeply inelastic scattering*, *Phys. Rev. D* **73** (2006) 014021, [hep-ph/0509076].

[90] W. Vogelsang and F. Yuan, *Single-transverse spin asymmetries: From DIS to hadronic collisions*, *Phys. Rev. D* **72** (2005) 054028, [hep-ph/0507266].

[91] M. Anselmino, M. Boglione, U. D'Alesio, A. Kotzinian, S. Melis, F. Murgia et al., *Sivers Effect for Pion and Kaon Production in Semi-Inclusive Deep Inelastic Scattering*, *Eur. Phys. J. A* **39** (2009) 89–100, [0805.2677].

[92] A. Bacchetta and M. Radici, *Constraining quark angular momentum through semi-inclusive measurements*, *Phys. Rev. Lett.* **107** (2011) 212001, [1107.5755].

[93] M. G. Echevarria, A. Idilbi, Z.-B. Kang and I. Vitev, *QCD Evolution of the Sivers Asymmetry*, *Phys. Rev. D* **89** (2014) 074013, [1401.5078].

[94] A. Bacchetta, F. Delcarro, C. Pisano and M. Radici, *The three-dimensional distribution of quarks in momentum space*, 2004.14278.

[95] J. C. Collins, *Fragmentation of transversely polarized quarks probed in transverse momentum distributions*, *Nucl. Phys. B* **396** (1993) 161–182, [hep-ph/9208213].

[96] F. Schlumpf, *Nucleon form-factors in a relativistic quark model*, *J. Phys. G* **20** (1994) 237–240, [hep-ph/9301233].

[97] B. Pasquini and S. Boffi, *Electroweak structure of the nucleon, meson cloud and light-cone wavefunctions*, *Phys. Rev. D* **76** (2007) 074011, [0707.2897].

[98] F. Schlumpf, *Charge form-factors of pseudoscalar mesons*, *Phys. Rev. D* **50** (1994) 6895–6898, [hep-ph/9406267].

[99] A. Metz, *Gluon-exchange in spin-dependent fragmentation*, *Phys. Lett. B* **549** (2002) 139–145, [hep-ph/0209054].

[100] L. P. Gamberg, G. R. Goldstein and K. A. Oganessyan, *A Mechanism for the T odd pion fragmentation function*, *Phys. Rev. D* **68** (2003) 051501, [hep-ph/0307139].

[101] J. C. Collins and A. Metz, *Universality of soft and collinear factors in hard-scattering factorization*, *Phys. Rev. Lett.* **93** (2004) 252001, [hep-ph/0408249].

[102] L. Gamberg, A. Mukherjee and P. Mulders, *Spectral analysis of gluonic pole matrix elements for fragmentation*, *Phys. Rev. D* **77** (2008) 114026, [0803.2632].

[103] S. J. Brodsky, D. S. Hwang and I. Schmidt, *Final state interactions and single spin asymmetries in semiinclusive deep inelastic scattering*, *Phys. Lett. B* **530** (2002) 99–107, [hep-ph/0201296].

[104] X.-d. Ji and F. Yuan, *Parton distributions in light cone gauge: Where are the final state interactions?*, *Phys. Lett. B* **543** (2002) 66–72, [hep-ph/0206057].

[105] G. R. Goldstein and L. Gamberg, *Transversity and meson photoproduction*, in *31st International Conference on High Energy Physics*, pp. 452–454, 9, 2002. hep-ph/0209085.

[106] L. P. Gamberg, G. R. Goldstein and K. A. Oganessyan, *Novel transversity properties in semiinclusive deep inelastic scattering*, *Phys. Rev. D* **67** (2003) 071504, [hep-ph/0301018].

[107] D. Boer, S. J. Brodsky and D. S. Hwang, *Initial state interactions in the unpolarized Drell-Yan process*, *Phys. Rev. D* **67** (2003) 054003, [hep-ph/0211110].

[108] M. Hirai, S. Kumano and M. Miyama, *Numerical solution of Q**2 evolution equation for the transversity distribution Delta(T)q*, *Comput. Phys. Commun.* **111** (1998) 150–166, [hep-ph/9712410].

[109] A. V. Efremov, P. Schweitzer, O. V. Teryaev and P. Zavada, *The relation between TMDs and PDFs in the covariant parton model approach*, *Phys. Rev.* **D83** (2011) 054025, [1012.5296].

[110] P. Schweitzer, M. Strikman and C. Weiss, *Intrinsic transverse momentum and parton correlations from dynamical chiral symmetry breaking*, *JHEP* **01** (2013) 163, [1210.1267].

[111] J. C. Collins, *Leading twist single transverse-spin asymmetries: Drell-Yan and deep inelastic scattering*, *Phys. Lett. B* **536** (2002) 43–48, [hep-ph/0204004].

[112] S. J. Brodsky, D. S. Hwang and I. Schmidt, *Initial state interactions and single spin asymmetries in Drell-Yan processes*, *Nucl. Phys. B* **642** (2002) 344–356, [hep-ph/0206259].

[113] E.-C. Aschenauer et al., *The RHIC SPIN Program: Achievements and Future Opportunities*, 1501.01220.

[114] STAR collaboration, L. Adamczyk et al., *Measurement of the transverse single-spin asymmetry in $p^{\uparrow} + p \to W^{\pm}/Z^0$ at RHIC*, *Phys. Rev. Lett.* **116** (2016) 132301, [1511.06003].

[115] M. Anselmino, M. Boglione, U. D'Alesio, F. Murgia and A. Prokudin, *Study of the sign change of the Sivers function from STAR Collaboration W/Z production data*, *JHEP* **04** (2017) 046, [1612.06413].

[116] A. Efremov, K. Goeke, S. Menzel, A. Metz and P. Schweitzer, *Sivers effect in semi-inclusive DIS and in the Drell-Yan process*, *Phys. Lett. B* **612** (2005) 233–244, [hep-ph/0412353].

[117] J. Collins, A. Efremov, K. Goeke, M. Grosse Perdekamp, S. Menzel, B. Meredith et al., *Sivers effect in Drell Yan at RHIC*, *Phys. Rev. D* **73** (2006) 094023, [hep-ph/0511272].

[118] M. Anselmino, M. Boglione, U. D'Alesio, S. Melis, F. Murgia and A. Prokudin, *Sivers effect in Drell-Yan processes*, *Phys. Rev. D* **79** (2009) 054010, [0901.3078].

[119] D. Boer, *Investigating the origins of transverse spin asymmetries at RHIC*, *Phys. Rev. D* **60** (1999) 014012, [hep-ph/9902255].

[120] NA10 collaboration, M. Guanziroli et al., *Angular Distributions of Muon Pairs Produced by Negative Pions on Deuterium and Tungsten*, *Z. Phys. C* **37** (1988) 545.

[121] J. Conway et al., *Experimental Study of Muon Pairs Produced by 252-GeV Pions on Tungsten*, *Phys. Rev. D* **39** (1989) 92–122.

[122] V. Barone, S. Melis and A. Prokudin, *Azimuthal asymmetries in unpolarized Drell-Yan processes and the Boer-Mulders distributions of antiquarks*, *Phys. Rev. D* **82** (2010) 114025, [1009.3423].

[123] COMPASS collaboration, B. Parsamyan, *Transversely polarized Drell-Yan measurements at COMPASS*, *PoS* **DIS2019** (2019) 195, [1908.01727].

[124] NuSea collaboration, L. Zhu et al., *Measurement of Angular Distributions of Drell-Yan Dimuons in $p + d$ Interaction at 800-GeV/c*, *Phys. Rev. Lett.* **99** (2007) 082301, [hep-ex/0609005].

[125] NuSea collaboration, L. Zhu et al., *Measurement of Angular Distributions of Drell-Yan Dimuons in $p + p$ Interactions at 800-GeV/c*, *Phys. Rev. Lett.* **102** (2009) 182001, [0811.4589].

[126] M. Burkardt and B. Hannafious, *Are all Boer-Mulders functions alike?*, *Phys. Lett. B* **658** (2008) 130–137, [0705.1573].

[127] P. Pobylitsa, *Transverse momentum dependent parton distributions in large N(c) QCD*, hep-ph/0301236.

[128] A. Sissakian, O. Shevchenko, A. Nagaytsev, O. Denisov and O. Ivanov, *Transversity and its accompanying T-odd distribution from Drell-Yan processes with pion-proton collisions*, *Eur. Phys. J. C* **46** (2006) 147–150, [hep-ph/0512095].